Proc. 23rd Winter Workshop on Nuclear Dynamics (2007) 000–000

23rd Winter Workshop on Nuclear Dynamics
Big Sky, Montana, USA
February 11–18, 2007

Topological reconstruction of open charm mesons using electron tagging

André Mischke[1] for the STAR Collaboration

[1] Institute for Subatomic Physics, Utrecht University, Princetonplein 5, 3584 CC Utrecht, The Netherlands

Abstract. We present first results on the topological reconstruction of open charm mesons in p+p collisions at $\sqrt{s_{\rm NN}}$ = 200 GeV using electron tagging. The analysis makes use of the full acceptance of the STAR electromagnetic calorimeter during Run VI data taking. A clear D^0 signal is obtained with a remarkable signal-to-background ratio of about 1/7 and a signal significance of about 4. The azimuthal correlation distribution of the subleading electrons associated with open charm mesons exhibits a two-peak structure. We found first indications for prompt charm meson pair production. This correlation technique allows detailed energy loss measurements of open charm mesons in heavy-ion collisions.

Keywords: heavy-quark correlations, electron tagging, open charm meson reconstruction
PACS: 25.75Dw, 25.75.-q, 25.75.Gz, 13.20.Fc, 13.20.He

1. Introduction

Measurements at the Relativistic Heavy-Ion Collider (RHIC) at Brookhaven National Laboratory have revealed a strong modification of the jet structure inside the created medium. Theoretical models, that attribute the jet attenuation to the energy loss of partons in the medium, have successfully described the present results for light-quark hadrons [1, 2] leading to the conclusion that the medium is indeed a plasma of quarks and gluons, but it behaves like a "perfect" fluid rather than an ideal gas [3]. Due to the limited sensitivity of the used probes, the conclusions are qualitative rather than quantitative. More details on the jet modification in the medium are needed and important aspects of the jet-quenching theory are as yet untested.

Heavy quarks (charm, bottom) are an optimal tool to study the medium properties since they are primarily produced in the early stage of the collision [3] and,

therefore, probe the complete space-time evolution of the medium. Due to their large mass ($m > 1$ GeV/c^2) their interaction processes can be calculated in pQCD. Heavy-quark hadrons live much longer ($c\tau = 100 - 200$ μm and $400 - 500$ μm for charm and bottom, respectively) than the created medium and, therefore, decay outside the medium. Theoretical models predicted that heavy quarks should experience smaller energy loss than light quarks when propagating through the medium due to the mass-dependent suppression (called dead-cone effect) [5].

RHIC measurements in heavy-ion collisions, however, have shown [6] that the electron yield from semi-leptonic heavy-quark decays is strongly suppressed relative to properly scaled p+p collisions, usually quantified in the nuclear modification factor. This factor shows a similar amount of suppression as observed for light-quark hadrons. Energy loss models with reasonable input parameters [7, 8] do not explain the observed suppression. It has been shown that collisional energy loss for heavy quarks [9, 10] and collisional dissociation of heavy mesons in the medium [11] may be significant for heavy-ion collisions. Only theoretical models, which include energy loss from charm only, describe the present data reasonably well [8]. Since these measurements are sensitive to the sum of charm and bottom contributions, there is an urgent need to disentangle the relative contributions experimentally.

Recent results on measurements of the azimuthal angular correlations between electrons (from heavy-flavor decays) associated with charged hadrons have shown that the relative bottom contribution (B/(B+C)) to the non-photonic electron spectrum is about 40% at a transverse momentum of $p_{\rm T} = 5$ GeV/c [12]. The measured $p_{\rm T}$ dependence of the relative bottom contribution can be used to verify the input parameters for most of the energy loss models.

In this paper, first results on a different approach are presented which allow disentangling the charm and bottom contributions to the non-photonic electrons using azimuthal correlations of electrons and D^0 mesons.

2. Data analysis

The analysis is based on p+p collisions at $\sqrt{s_{\rm NN}} = 200$ GeV measured by the STAR experiment at RHIC. Particle identification via the specific energy loss (resolution $\sigma_{dEdx}/dEdx = 8\%$) and tracking over a large kinematical range with very good momentum resolution is performed by the Time Projection Chamber (TPC) [13]. The TPC is located inside a solenoidal magnet with a maximum field of 0.5T and has an acceptance of $|\eta| < 1.4$ and full azimuthal coverage. The STAR detector utilizes a barrel-electromagnetic calorimeter (BEMC) [14] as a leading particle (electrons, photons) trigger to study high-$p_{\rm T}$ particle production. The BEMC is a lead-scintillator sampling calorimeter with an energy resolution of $\delta E/E \approx 16\%/\sqrt{E}$. The calorimeter, situated behind the TPC, covers an acceptance of $|\eta| < 1$ and full azimuth. During Run VI data taking the full BEMC was installed and $\approx 97\%$ operational. To enhance the high $p_{\rm T}$ range, a high-tower trigger was used with an energy threshold of 5.4 GeV for the highest energy in a BEMC cell. The high-tower

trigger efficiency is nearly 100%.

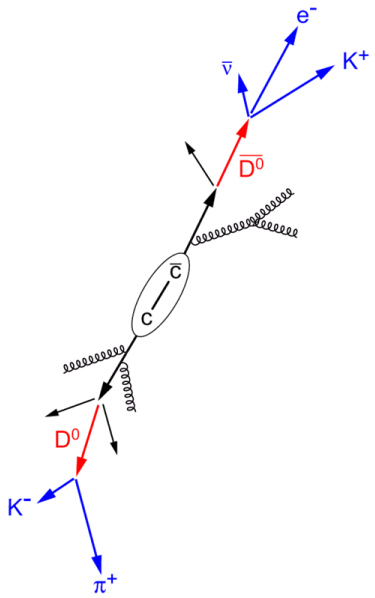

Fig. 1. Schematic view of the fragmentation of $c\bar{c}$ pair.

The integrated luminosity for p+p collisions during Run VI was 9 pb^{-1} of those 1.2 million events were used after event quality cuts (high-tower trigger and z-coordinate of the collision vertex (beam axis) within 30 cm of the TPC centre). The tight vertex cut is used to minimize the amount of material within the detector volume causing photon conversions.

Due to the large mass, heavy quarks can only be created in pairs such that each quark-antiquark pair is correlated in relative azimuth due to momentum conservation. These events are characterized by two back-to-back orientated sprays of particles leading to a two-peak structure in the azimuthal angular correlation distribution. These correlations survive the fragmentation process to a large extent in p+p interactions.

A new analysis method is used to identify events with heavy-quark production using the back-to-back decay topology of heavy-quark jets. As an example, Figure 1 shows a schematic view of the fragmentation of a $c\bar{c}$ pair. The first charm particle is identified by the subleading electron (trigger side) and the balancing charm quark is found by the open charm meson (probe side). The branching fraction for a semi-leptonic charm or bottom decay ($c, b \rightarrow l + X$) is $\approx 10\%$. Approximately

54% of the charm quarks decay into D^0 mesons. While triggering on the subleading electron, the second charm particle can be used to identify the underlying production mechanisms since, e.g., charm-quark pairs from flavor creation (LO) are oriented back-to-back in the azimuthal angular correlation distribution ($\Delta\phi = \pi$) whereas they are collinear ($\Delta\phi = 0$) for gluon splitting (NLO) processes. An additional charm contribution on the near-side is expected from bottom decays.

In the following sections, the identification of the non-photonic electron trigger and the reconstruction of the D^0 mesons are described in detail.

2.1. Electron identification

The electron identification is performed by combining the information from the TPC (track momentum and ionization energy loss (dE/dx)) and the BEMC (cell energy). Candidate tracks are selected having a pseudo-rapidity of $|\eta| < 1$. Due to the momentum resolution of the calorimeter, only particles with a transverse momentum of $p_{\mathrm{T}} > 1.5$ GeV/c can be measured.

A shower maximum detector, located approximately at a depth of 5 radiation length inside the calorimeter modules, measures the profile of an electromagnetic shower and the position of the shower maximum with high resolution $(\Delta\eta, \Delta\phi) = (0.007, 0.007)$. In contrast to hadrons, electrons deposit most of their energy in the BEMC cells. A cut on the shower profile size combined with a requirement on the ratio of momentum-to-cell energy, $0 < p/E < 2$, reject a large amount of hadrons. The final electron sample is selected by applying a momentum dependent cut on the ionization energy loss (about $3.5 < dE/dx < 5.0$ keV/cm). More details on the electron reconstruction can be found in Ref. [6].

The resulting hadron suppression factor is 10^5 at $p_{\mathrm{T}} = 2$ GeV/c and 10^2 at $p_{\mathrm{T}} = 7$ GeV/c. The electron purity is $\approx 100\%$ at $p_{\mathrm{T}} = 5$ GeV/c and decreases to about 70% at $p_{\mathrm{T}} = 12$ GeV/c.

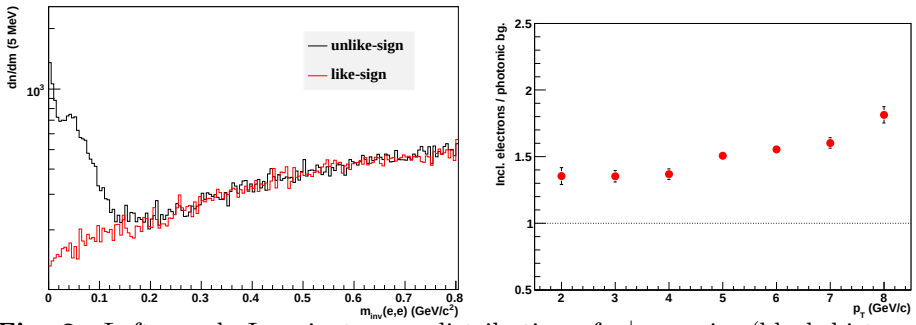

Fig. 2. Left panel: Invariant mass distribution of e^+e^- pairs (black histogram) and the combinatorial background using like-sign electron pairs (red histogram). Right panel: Ratio of inclusive electrons to the photonic background as a function of electron trigger p_{T}. Statistical errors are shown only.

Most of the electrons are originating from other sources than heavy-flavor decays. Photon conversions ($\gamma \rightarrow e^+e^-$) in the detector material between the interaction point and the TPC and neutral pion and η Dalitz decays ($\pi^0, \eta \rightarrow e^+e^-\gamma$) represent the dominant source of photonic electrons. Photonic electron contributions from other decays, like ρ, ϕ and Ke3, are small and can be neglected. Electrons from the photonic background can be determined by calculating the invariant mass of electron pairs. Here, each electron candidate is combined with tracks within the TPC acceptance which are passing loose cuts on the ionization energy loss to preselect electron candidates.

The resulting invariant mass distribution of unlike-sign electron pairs is illustrated in the left panel of Figure 2. The fraction of random pairs with a non-photonic electron can be estimated using like-sign pair combinations. The peak at zero invariant mass arises from conversions and the tail at low invariant mass is due to Dalitz decays [15]. Electrons with an invariant mass of $m < 150$ MeV/c^2 are disregarded. The photonic background finding efficiency, using this method, is $\approx 70\%$.

The right panel of Figure 2 shows the p_{T} dependence of the ratio of inclusive electrons to the photonic background. A significant excess of non-photonic electrons is observed which increases with increasing p_{T}. A total of ≈6k non-photonic electrons, originating mostly from heavy-flavor decays, are obtained for the further analysis.

2.2. D^0 reconstruction

The associated D^0 mesons are reconstructed in the hadronic decay channel $\mathrm{D}^0 \rightarrow \mathrm{K}^-\pi^+$ (branching fraction 3.84 %) by calculating the invariant mass of all oppositely charged TPC track combinations (unlike-sign pairs) in the same event. Up to now, the precise D^0 decay topology can not be resolved due to insufficient tracking resolution close to the collision vertex. A dE/dx cut of $\pm 3\sigma$ around the Kaon band is applied on the negative tracks. The resulting track sample is called Kaon candidates. Due to the high abundance of pions in the collisions, one usually has to handle a large combinatorial background of random pair combinations [16]. Therefore, in this analysis, events with a non-photonic electron trigger only are used for the D^0 reconstruction. Furthermore, the Kaon candidates have to have the same sign as the non-photonic electrons.

The resulting invariant mass distribution of (K, π) pairs shows a clear D^0 peak (Figure 3, left panel). The combinatorial background of random pairs is evaluated by combining all like-sign charged tracks in the same event. The discrepancy of the shape between the invariant mass and the combinatorial background distribution at lower masses is due to jet particle correlations which are not included in the background evaluation. The invariant mass distribution without a non-photonic electron trigger does not have a signal for the used track quality cuts. The non-photonic electron trigger allows suppressing the combinatorial background significantly (by a factor of ≈ 100 compared to earlier results [16]) yielding a signal-to-background ratio of about 1/7. A signal significance of approximately 4 is obtained.

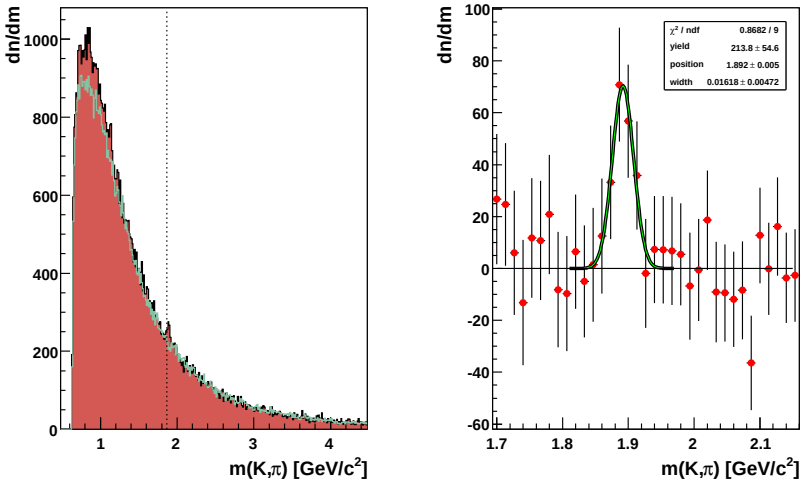

Fig. 3. Left panel: Invariant mass distribution of (K, π) pairs requiring a non-photonic electron trigger in the event (red histogram) and the combinatorial background using like-sign (K, π) pairs (green histogram). Right panel: Background subtracted invariant mass distribution. The solid black line is a Gaussian fit to the data around the peak region.

In the right panel of Figure 3, the background subtracted invariant mass distribution is illustrated. The peak position and width are obtained using a Gaussian fit to the data. The measured peak position, $m = 1.892 \pm 0.005$ GeV/c^2, is slightly higher than the PDG value of 1.864 GeV/c^2 which can be explained by the finite momentum resolution of the TPC. The width of the signal, $\sigma_m = 16 \pm 5$ MeV/c^2, is found to be similar to earlier results and expectations from MC simulations [16]. Within statistical uncertainties, the D^0 and $\overline{D^0}$ yields are equal.

2.3. Electron−D^0 meson azimuthal correlation

The azimuthal angular ($\Delta\phi$) correlation is calculated between the transverse momentum of the non-photonic electron triggers and the associated charged hadron-pairs. The (K, π) invariant mass distribution is calculated for different $\Delta\phi$ bins and the yield of the associated D^0 mesons is extracted as the area underneath a Gaussian fit to the signal. Figure 4 shows the e−D^0 azimuthal correlation distribution. In the following, we imply electron−D^0 and positron−anti-D^0 pairs when using e−D^0 unless otherwise specified.

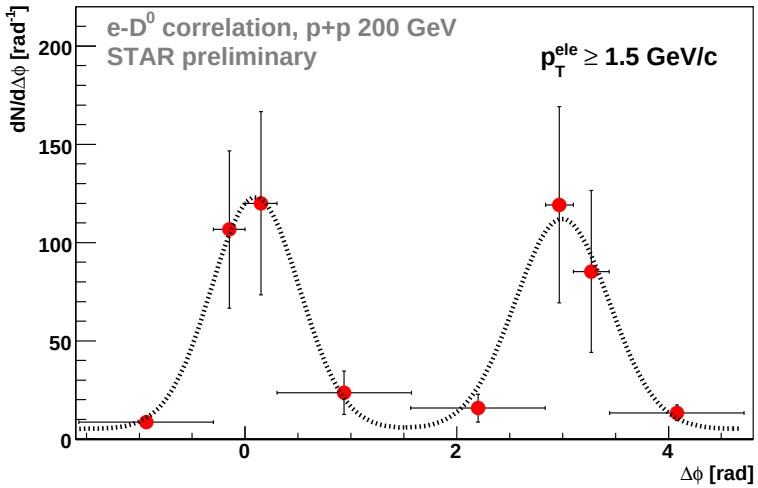

Fig. 4. Azimuthal angular correlation distribution of non-photonic electrons and D^0 mesons in p+p collisions at $\sqrt{s_{\rm NN}} = 200$ GeV (trigger $p_{\rm T} \geq 1.5$ GeV/c). Statistical errors are shown only. To guide the eye, the dotted line illustrates a two-Gaussian plus constant fit to the data.

3. Results

The e$-$D^0 azimuthal correlation distribution exhibits a near- and away-side correlation peak with similar yields. The data shows indications for prompt charm meson pair production leading to the back-to-back correlation peak ($\Delta\phi = \pi$). The near-side correlation peak can be interpreted by contributions from gluon splitting and bottom decays. The CDF collaboration obtained a similar correlation pattern for $D^0(D^+)-D^{*-}$ pairs in p+$\overline{\rm p}$ collisions at $\sqrt{s_{\rm NN}} = 1.96$ TeV at the Tevatron Collider at Fermilab [17]. Their measurements have shown that gluon splitting ($\Delta\phi = 0$) is as important as flavor creation processes ($\Delta\phi = \pi$). Related studies have yet to be performed using these data and event generators such as Pythia and Herwig to obtain the relative contributions at RHIC energies.

4. Conclusions

This work presents the first heavy-flavor correlation measurement at RHIC. The particular advantage of the presented correlation method, in contrast to conventional open charm measurements, is the possibility to trigger on collisions with heavy-quark production using the decay electrons.

The azimuthal correlation distribution between non-photonic electrons associ-

ated with open charm mesons exhibits a two-peak structure. The away-side correlation peak can be explained by prompt charm meson pair production whereas the near-side peak represents contributions from gluon splitting and bottom decays. The results are in qualitative agreement with recent CDF measurements. Dedicated event generators, like Pythia or Herwig, are needed to disentangle the charm and bottom contribution to the azimuthal correlation distribution.

The presented, new correlation technique has the potential for detailed energy loss measurement of open charm mesons in heavy-ion collisions in the future.

Acknowledgments

The author is grateful for the support by the Nederlands Organisation for Scientific Research (NWO).

References

1. X.-N. Wang, *Phys. Lett.* **B595** (2004) 165.
2. I. Vitev and M. Gyulassy, *Phys. Rev. Lett.* **89** (2002) 252302.
3. B. I. Abelev et al. (STAR Collaboration), *Nucl. Phys.* **A757** (2005) 102.
4. Z. Lin and M. Gyulassy, *Phys. Rev.* **C51** (1995) 2177.
5. Y. L. Dokshitzer and D. E. Kharzeev, *Phys. Lett.* **B519** (2001) 199.
6. B. I. Abelev et al. (STAR Collaboration), *Phys. Rev. Lett.* in press (arXiv: nucl-ex/0607012).
7. M. Djordjevic et al., *Phys. Lett.* **B632** (2006) 81.
8. N. Armesto et al., *Phys. Lett.* **B637** (2006) 362.
9. S. Wicks et al., *Nucl. Phys.* **A784** (2007) 426.
10. H. van Hees, V. Greco and R. Rapp, *Phys. Rev.* **C 73** (2006) 034913.
11. A. Adil and I. Vitev, arXiv: hep-ph/0611109.
12. X. Lin et al. (STAR Collaboration), submitted to *J. Phys. G* (arXiv: nucl-ex/0701050).
13. M. Anderson et al. (STAR Collaboration), *Nucl. Instr. Meth.* **A499** (2003) 659.
14. M. Beddo et al. (STAR Collaboration), *Nucl. Instr. Meth.* **A499** (2003) 725.
15. S. Eidelman et al., *Phys. Lett.* **B592** (2004), 1.
16. J. Adams et al. (STAR Collaboration), *Phys. Rev. Lett.* **94** (2005) 062301.
17. B. Reisert et al. (CDF Collaboration), Beauty 2006, to be published in *Nucl. Phys. B (Proc. Suppl.).*